Int. J. Solids Structures, 1969, Vol. 5, pp. 879 to 892. Pergamon Press. Printed in Great Britain

STRESSES AT THE INTERSECTION OF TWO CYLINDRICAL SHELLS OF EQUAL DIAMETER

M. V. V. MURTHY

National Aeronautical Laboratory, Bangalore, India

Abstract—The stresses at the intersection of two cylindrical shells of equal diameter, joined over a plane elliptic face and subjected to internal pressure, are analysed. The results are valid for all possible values of the angle between axes of the two shells. Errors of the order of $(h/a)^{\frac{1}{2}}$ are admitted, where h and a denote thickness and radius of the shells respectively. Results are given in the form of simple formulae for stresses near the plane of intersection. A graph is given from which the stress concentration factor, based on distortion energy, can be directly read over a wide range of parameters.

NOTATION

$2a, h$	mean diameter and thickness respectively of either shell
2α	angle between axes of the two shells (Fig. 1)
λ	$= \tan \alpha$
E	Young's modulus
ν	Poisson's ratio
β	$= [3(1-\nu^2)]^{\frac{1}{4}}(a/h)^{\frac{1}{2}}$
p	uniform internal pressure
x	distance, measured from a plane normal to shell axis (Fig. 2) and non-dimensionalized through a
θ	angular coordinate (Fig. 2)
z	distance from the plane of intersection, measured parallel to shell axis (Fig. 2) and non-dimensionalized through a
μ	$= [3(1-\nu^2)]^{\frac{1}{4}}(a/h)^{\frac{1}{2}}(1+\lambda^2 \sin^2 \theta)^{-1}$
ψ	obliqueness of local tangent (Fig. 3)
$\bar{z}$	normal distance measured from the oblique edge (Fig. 3) and non-dimensionalized through a
$\bar{\theta}$	θ coordinate at the foot of normal to the oblique edge (Fig. 3)
ξ, η	directions, on the middle surface of the shell, perpendicular to and along the line z = constant
$N_x, N_\theta, N_{x\theta}$	membrane stress resultant forces (Fig. 4) non-dimensionalized through pa
$M_x, M_\theta, M_{x\theta}$	stress resultant couples (Fig. 4) non-dimensionalized through pah
Q_x, Q_θ	transverse shear forces (Fig. 4) non-dimensionalized through pa
U, V, W	displacement components (Fig. 2) in the axial, circumferential and radial directions respectively, non-dimensionalized through pa^2/Eh
Φ	stress function
F	complex stress-displacement function $(W+i\Phi)$, where $i = \sqrt{-1}$
$\sigma_\xi, \sigma_\eta, \tau_{\xi\eta}$	stresses in ξ and η directions, non-dimensionalized through pa/h (Fig. 4)

1. INTRODUCTION

IN THIS paper, analytical solutions are presented for stresses around the unreinforced intersection of two, long, thin circular cylindrical shells of equal diameter joined over a plane elliptic face and subjected to uniform hydrostatic pressure (Fig. 1). This problem is of considerable practical importance, because it is encountered frequently in high

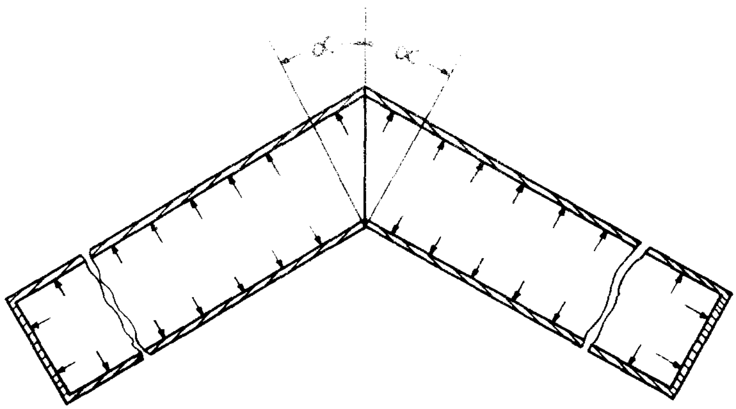

FIG. 1. Pressurized junction of two cylindrical shells.

pressure pipe lines. The ends of the two shells are assumed to be closed and situated far away from the plane of intersection. Free displacements are allowed and no restriction is placed on the value of α. Throughout this paper, terms of order $1/\beta$ are neglected in comparison with unity. In other words, errors of order $(h/a)^{\frac{1}{2}}$ are admitted.

The earliest attempt on the theoretical solution of a related problem was made by Kornecki [1]. Kornecki considered the problem of a cylindrical shell subjected to uniform pressure and clamped along an oblique end section. Corum [2] carried out an analysis of the same problem for seven different loading cases, namely internal pressure* and three mutually perpendicular moments and perpendicular forces applied at the free end. Results of extensive experimental work are also given in Corum's paper. The problems considered by Kornecki [1] and Corum [2] are equivalent to the problem of two cylindrical shells joined over an elliptic face and reinforced by an infinitely rigid ring along the line of intersection. This paper deals with the problem of unreinforced intersection, which is different from those of both Kornecki and Corum.

The problem treated here has been examined earlier in references [3]–[5]. Van der Neut's solution [3], although valid for all values of α and carried to the same degree of approximation as this analysis, leads to an impossible state of stress at $x = \infty$. The solutions in references [4] and [5] are restricted to small values of α and lead to exactly identical results. In reference [4], the method of three dimensional linear elasticity is used, whereas the solution given in reference [5] is based on a shell theory approach.

Van der Neut's solution [3] leads to the conclusion that the longitudinal membrane forces at $x = \infty$ should be of the form

$$N_x = \tfrac{1}{2}(1+\lambda^2 \cos 2\theta). \tag{1}$$

It should be noted that N_x, in equation (1), is nondimensionalized as indicated in the Notation. Evidently, equation (1) has to be rejected mathematically, because we know from shell theory that any stress system with a sinusoidal variation† along the circumference of a cylindrical shell can only vary exponentially in the axial direction and cannot remain constant.

* For the case of internal pressure, the results of Corum are identical with those of Kornecki [1].

† Except the zero and first harmonics.

In Van der Neut's analysis, only the rapidly decaying stress system is considered to satisfy the boundary conditions. The shell equations have another type of solution corresponding to a slowly decaying stress system with a larger decay length. It is shown in this analysis that by taking this into account, the anomalous stress distribution, as in equation (1), can be avoided and a completely satisfactory solution can be obtained to the degree of approximation stated. In references [4] and [5], although only rapidly decaying stresses are considered, this inconsistency does not show up, because α is taken to be small and λ^2 is neglected everywhere in comparison with unity. Equation (1) then yields the classical value for N_x at $x = \infty$.

2. GOVERNING EQUATIONS AND BOUNDARY CONDITIONS

All distances, stresses, stress resultant forces, stress resultant couples and displacements in this analysis are non-dimensionalized through a, pa/h, pa, pah and pa^2/Eh respectively.

We define a "residue problem" as the stress problem of the cylindrical shell subjected to certain edge loads at $z = 0$, which produce stresses decaying to zero as $z \to \infty$ and which, if added to the uniform stress field due to internal pressure

$$\bar{N}_x = \tfrac{1}{2}, \qquad \bar{N}_\theta = 1, \qquad \bar{N}_{x\theta} = 0 \tag{2)–(4}$$

satisfy the required boundary conditions at the plane of intersection. In the following analysis, a solution is obtained for this residue problem and subsequently added to the uniform state of stress, equations (2)–(4).

2.1 *Governing equations*

The governing equations used are Donnel's equations for circular cylindrical shells. The original Donnel's equations [6] are in the form of three equations for the three displacement components U, V and W. It is possible to reduce these three equations to a single equation for F, which, in the absence of normal pressure, can be written in the following form. It should be noted that the normal pressure is taken to be zero, because here we solve the residue problem, which is only an edge load problem.

$$\nabla^4 F(x, \theta) + 2i\beta^2 \frac{\partial^2 F(x, \theta)}{\partial x^2} = 0 \tag{5}$$

where

$$\nabla^4 = \left(\frac{\partial^2}{\partial x^2} + \frac{\partial^2}{\partial \theta^2}\right)^2$$

and the stress resultants can be determined from F by using the relations

$$N_x = -\frac{1}{2\beta^2} \frac{\partial^2 \Phi(x, \theta)}{\partial \theta^2} \tag{6}$$

$$N_\theta = -\frac{1}{2\beta^2} \frac{\partial^2 \Phi(x, \theta)}{\partial x^2} \tag{7}$$

$$N_{x\theta} = \frac{1}{2\beta^2} \frac{\partial^2 \Phi(x, \theta)}{\partial x \partial \theta} \tag{8}$$

$$M_x = \frac{1}{2\beta^2[12(1-\nu^2)]^{\frac{1}{2}}}\left[\frac{\partial^2 W(x,\theta)}{\partial x^2} + \nu\frac{\partial^2 W(x,\theta)}{\partial \theta^2}\right] \tag{9}$$

$$M_\theta = \frac{1}{2\beta^2[12(1-\nu^2)]^{\frac{1}{2}}}\left[\frac{\partial^2 W(x,\theta)}{\partial \theta^2} + \nu\frac{\partial^2 W(x,\theta)}{\partial x^2}\right] \tag{10}$$

$$M_{x\theta} = \frac{(1-\nu)}{2\beta^2[12(1-\nu^2)]^{\frac{1}{2}}}\frac{\partial^2 W(x,\theta)}{\partial x \partial \theta} \tag{11}$$

$$Q_x = \frac{1}{4\beta^4}\left[\frac{\partial^3 W(x,\theta)}{\partial x^3} + \frac{\partial^3 W(x,\theta)}{\partial x \partial \theta^2}\right] \tag{12}$$

$$Q_\theta = \frac{1}{4\beta^4}\left[\frac{\partial^3 W(x,\theta)}{\partial x^2 \partial \theta} + \frac{\partial^3 W(x,\theta)}{\partial \theta^3}\right]. \tag{13}$$

Sign conventions for the stress resultants are shown in Fig. 4.

2.2 *Boundary conditions*

Figure 5 shows the trace of middle surface of the shell on the plane of intersection. S_1 and S_2 denote shear forces per unit length, acting in the plane of intersection in directions parallel to the major and minor axes of the ellipse. M_{12} denotes the twisting moment per unit length of the elliptic boundary and vector M_{12} is normal to the plane of intersection. Since the plane of intersection is also a plane of symmetry, it follows that there can be no shearing stresses in the plane of intersection and S_1, S_2 and M_{12} should vanish individually; i.e.

$$S_1 = 0, \qquad S_2 = 0, \qquad M_{12} = 0. \tag{14)–(16}$$

The other boundary conditions follow from the deformation of the plane of intersection. From symmetry considerations, rotation of the middle surface of the shell in a direction normal to the edge should be zero:

$$\left[\frac{\partial W(\bar{z},\bar{\theta})}{\partial \bar{z}}\right]_{\bar{z}=0} = 0. \tag{17}$$

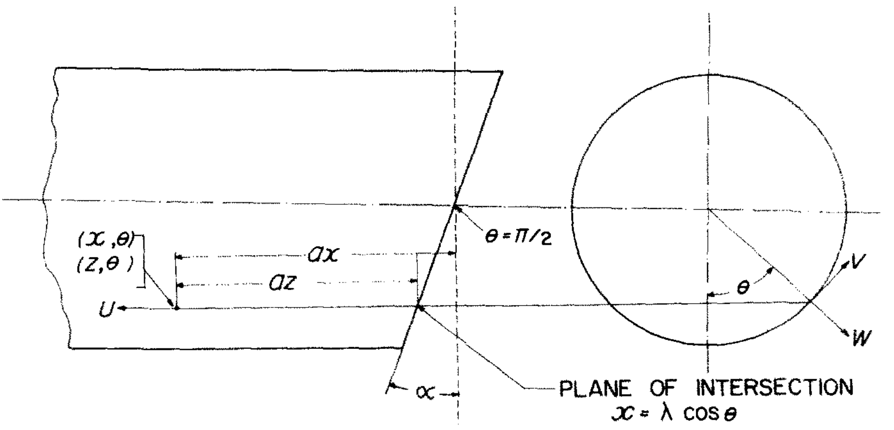

FIG. 2. Middle surface of shell.

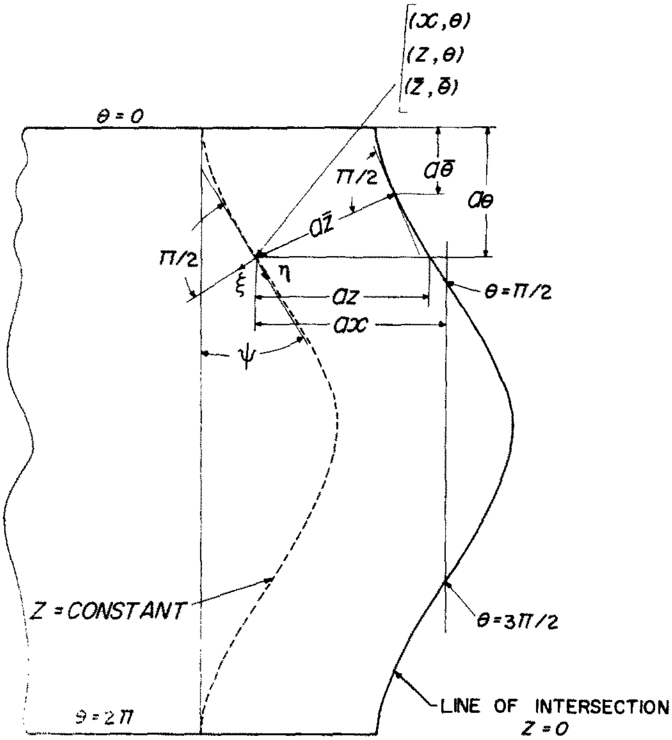

FIG. 3. Shell developed on a plane.

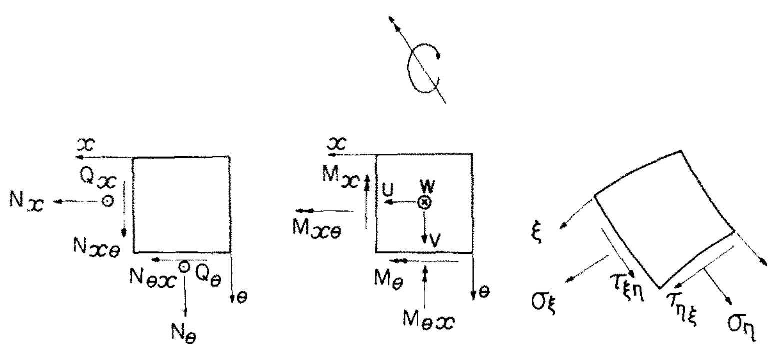

FIG. 4. Stresses and stress resultants. ⊙—Downward; ⊗—Upward.

Another condition, which follows from symmetry, is that all points on the plane of intersection should remain to be in a plane even after loading. In other words, if the structure is restrained against rigid body displacement and rotation, the displacement component normal to the plane of intersection should vanish. This means

$$\left[\lambda(W\cos\theta - V\sin\theta) - U + \frac{(1+\nu)}{2}\lambda\cos\theta\right]_{\bar{z}=0} = 0. \tag{18}$$

The last term in the foregoing equation arises from the uniform stresses, equations (2)–(4).

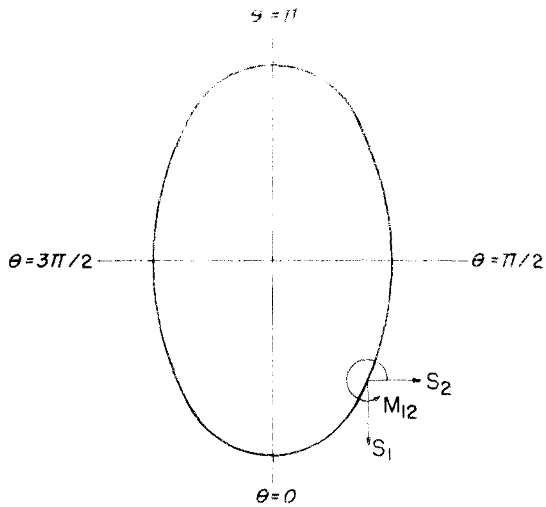

FIG. 5. Middle line of elliptic interface.

We have five boundary conditions (14)–(18), whereas the governing equation is only of the fourth order. The usual way of overcoming this difficulty is to replace the three conditions (14)–(16) by only two equations, using the Kirchhoff shear type of boundary condition. But, in this particular analysis, the five boundary conditions are retained as they are, because it is found that, by a coincidence, all these five conditions can be satisfied to the degree of accuracy to which this analysis is carried. But if one likes to proceed to a higher approximation, the Kirchhoff shear must be introduced.

S_1, S_2 and M_{12} can be expressed in terms of stress resultant forces and couples by the relations

$$S_1 = \cos\psi\cos\alpha\left[-\lambda\left(\tfrac{1}{2}+N_x+N_{x\theta}\lambda\sin\theta\right)+\cos\theta(Q_x+Q_\theta\lambda\sin\theta) + \sin\theta\{N_{x\theta}+\lambda\sin\theta(1+N_\theta)\}\right]_{z=0}, \tag{19}$$

$$S_2 = \cos\psi[\sin\theta(Q_x+Q_\theta\lambda\sin\theta)-\cos\theta\{N_{x\theta}+\lambda\sin\theta(1+N_\theta)\}]_{z=0}, \tag{20}$$

$$M_{12} = \cos\psi\cos\alpha[M_{x\theta}(\lambda^2\sin^2\theta-1)+\lambda\sin\theta(M_x-M_\theta)]_{z=0}. \tag{21}$$

The quantities $\frac{1}{2}$ and unity, adjacent to N_x and N_θ respectively, in equations (19) and (20) correspond to the uniform stresses, equations (2)–(4). ψ represents the obliqueness of local tangent (Fig. 3) and

$$\tan\psi = \lambda\sin\theta. \tag{22}$$

3. SOLUTION

Equation (5) can be split into two equations of second order:

$$\nabla^2 F_1(x,\theta)-(1-i)\beta\frac{\partial F_1(x,\theta)}{\partial x} = 0 \tag{23}$$

$$\nabla^2 F_2(x,\theta)+(1-i)\beta\frac{\partial F_2(x,\theta)}{\partial x} = 0. \tag{24}$$

By separation of variables, solution of equation (23) can be written as

$$F_1 = \sum_{n=0,1,2,\ldots}^{\infty} (A_n + iB_n)\,e^{k_n x}\cos n\theta. \tag{25}$$

Only cosine terms in θ are chosen in equation (25), because the stress system should be even in θ. A_n, B_n are real constants and

$$k_n = \tfrac{1}{2}[(1-i)\beta \pm (4n^2 - 2i\beta^2)^{\frac{1}{2}}]. \tag{26}$$

k_n has, therefore, two roots; the real part of one root is positive, whereas the real part of the other root is negative. We have to select only that root for which the real part is negative, because stresses in the residue problem should tend to zero as $z \to \infty$. We now make an assumption that the boundary conditions can be satisfied with the first few values of n in equation (25). It will be actually found during the process of satisfying the boundary conditions that we need, in fact, only one term in equation (25) corresponding to $n = 2$. For small values of n, k_n from equation (26) can be written as

$$k_n = -\frac{(1+i)n^2}{\beta}\left[1 - \frac{i}{2}\left(\frac{n}{\beta}\right)^2 - \frac{1}{2}\left(\frac{n}{\beta}\right)^4 + \ldots\right] = O(1/\beta). \tag{27}$$

We write A_n and B_n also in powers of $1/\beta$

$$(A_n + iB_n) = [A_{n(0)} + iB_{n(0)}] + \frac{1}{\beta}[A_{n(1)} + iB_{n(1)}] + \frac{1}{\beta^2}[A_{n(2)} + iB_{n(2)}] + \ldots. \tag{28}$$

Since the edge loads are applied at $z = 0$, it is convenient to work with the oblique coordinates (z, θ). z and x are connected by the relationship (see Fig. 2)

$$z = x - \lambda\cos\theta. \tag{29}$$

By means of equations (27)–(29), we can write equation (25) in the form

$$F_1 = \left[\sum \{A_{n(0)} + iB_{n(0)}\}\,e^{k_n z}\cos n\theta\right] + O(1/\beta). \tag{30}$$

The symbol Σ in the foregoing equation denotes summation over small values of n except $n = 0$. The term corresponding to $n = 0$ is excluded, because it is a trivial case, as it can be seen from equation (27).

We do not seek the solution of equation (24) in the form of Fourier series as we did for equation (23), because this leads to certain mathematical difficulties in satisfying the boundary conditions.

Equation (24) can be written in (z, θ) as

$$\frac{\partial^2 F_2(z,\theta)}{\partial z^2}(1 + \lambda^2\sin^2\theta) + 2\frac{\partial^2 F_2(z,\theta)}{\partial z\,\partial\theta}\lambda\sin\theta + \frac{\partial F_2(z,\theta)}{\partial z}[\lambda\cos\theta + (1-i)\beta] + \frac{\partial^2 F_2(z,\theta)}{\partial\theta^2} = 0. \tag{31}$$

Following the lines of the method of asymptotic integration of shell equations developed by Gol'denveizer [7], the solution of equation (31) is taken in the form

$$F_2(z,\theta) = e^{\beta f(z,\theta)}\left[G_0(z,\theta) + \frac{1}{\beta}G_1(z,\theta) + \frac{1}{\beta^2}G_2(z,\theta) + \ldots\right] \tag{32}$$

where

$$f(0, \theta) = 0. \tag{33}$$

Substituting from equation (32) in equation (31), equating coefficients of β^2 on both sides and making use of equation (33), we get

$$\left(\frac{\partial f}{\partial z}\right)_{z=0} = (i-1)(1+\lambda^2 \sin^2\theta)^{-1}. \tag{34}$$

$G_0(z, \theta)$ is arbitrary, to be determined from boundary conditions. In the immediate neighbourhood of $z = 0$, we can write from equation (33)

$$f(z, \theta) \simeq z\left(\frac{\partial f}{\partial z}\right)_{z=0}$$

The real part of $f(z, \theta)$ is, therefore, negative, which is exactly what we expect because stresses in the edge load problem should decrease with increase in z. Apart from the solution we have just obtained, equation (24) being a second order equation has another solution; but this solution corresponds to stresses tending to infinity as $z \to \infty$, which is not of interest to us.

There is one point which is worth noticing here. F_1 represents a system of stresses which decay slowly as we move away from the edge, whereas F_2 corresponds to rapidly decaying stresses. The solution of the governing equation is taken as a linear combination of F_1 and F_2.

$$F = W + i\Phi = \beta^2 F_1 + \beta F_2. \tag{35}$$

The powers of β associated with F_1 and F_2 in equation (35) are determined by a few trials in satisfying the boundary conditions. From the original Donnel's equations [6] in U, V and W, we have

$$\nabla^4[U(x, \theta)] = -\nu\frac{\partial^3 W(x, \theta)}{\partial x^3} + \frac{\partial^3 W(x, \theta)}{\partial x\, \partial\theta^2} \tag{36}$$

$$\nabla^4[V(x, \theta)] = -(2+\nu)\frac{\partial^3 W(x, \theta)}{\partial x^2\, \partial\theta} - \frac{\partial^3 W(x, \theta)}{\partial\theta^3}. \tag{37}$$

W and Φ are obtained by separating the real and imaginary parts in equation (35). Substituting for W in equations (36) and (37), U and V are obtained.

With the aid of equations (19)–(21), (6)–(13) and (29), the boundary conditions (14)–(16) are expressed in terms of partial derivatives of W and Φ with respect to z and θ. The fourth boundary condition (17) is also expressed in z and θ. In the resulting four equations and in the last boundary condition (18), we now substitute for W, Φ, U and V derived as in the previous paragraph. In doing so, only terms involving the highest power of β are retained in each equation. Solution of these equations leads to

$$F_1 = i\frac{\lambda^2}{4} e^{k_2 z} \cos 2\theta + O(1/\beta). \tag{38}$$

$$G_0(0, \theta) = \tfrac{1}{2}\lambda \cos\theta(1-i)(1+\lambda^2 \sin^2\theta). \tag{39}$$

Actually, only four boundary conditions (14), (15), (17) and (18) are enough to determine the unknowns. The remaining boundary condition (16) is then automatically satisfied.

In determining the stresses, we will restrict ourselves to a narrow strip of width of the order of $\sqrt{ah}$ in the neighbourhood of the plane of intersection, i.e. a zone in which $z = 0(1/\beta)$. The reason is that we get simple expressions for stresses and after all, we are only interested in this critical zone, where the stresses are high. Taylor series expansions in z, in this zone yield

$$f(z, \theta) = z\left(\frac{\partial f}{\partial z}\right)_{z=0} + O(1/\beta^2) \tag{40}$$

$$\frac{\partial f(z, \theta)}{\partial z} = \left(\frac{\partial f}{\partial z}\right)_{z=0} + O(1/\beta) \tag{41}$$

$$G_0(z, \theta) = G_0(0, \theta) + O(1/\beta). \tag{42}$$

From equation (27), we get to a first approximation

$$k_2 = -\frac{4(1+i)}{\beta} + O\left(\frac{1}{\beta^2}\right). \tag{43}$$

4. RESULTS AND DISCUSSION

Stresses can be now determined to a first approximation. ξ and η represent the directions of principal stresses at the plane of intersection (see Fig. 3). It is, therefore, useful to derive expressions for stresses in these directions. By the usual transformation from equations (2)–(4), the uniform membrane stresses due to internal pressure in ξ and η directions can be obtained:

$$\bar{\sigma}_\xi = \frac{(1+2\lambda^2 \sin^2\theta)}{2(1+\lambda^2 \sin^2\theta)} \tag{44}$$

$$\bar{\sigma}_\eta = \frac{(2+\lambda^2 \sin^2\theta)}{2(1+\lambda^2 \sin^2\theta)} \tag{45}$$

$$\bar{\tau}_{\xi\eta} = \frac{\lambda \sin\theta}{2(1+\lambda^2 \sin^2\theta)}. \tag{46}$$

From equations (6)–(11), we can derive expressions for stress resultants in ξ and η directions in terms of partial derivatives of W and Φ with respect to z and θ. Substituting for W and Φ in these relations from equation (35) and making use of equations (32), (34) and (38)–(43), we arrive at the following formulae for stresses in the residue problem. In deriving these, only terms involving the highest power of β are retained in each expression, because we have ignored $1/\beta$ in comparison with unity throughout.

Stresses from the residue problem

$$\sigma_\xi(\text{membrane}) = \tfrac{1}{2}(1+\lambda^2 \sin^2\theta)^{-1}[\lambda^2 \cos 2\theta\, e^{-4z/\beta} \cos(4z/\beta) - \lambda^2 \cos^2\theta\, e^{-\mu z} \cos \mu z] \tag{47}$$

$$\sigma_\eta(\text{membrane}) = \tfrac{1}{2}\beta\lambda \cos\theta\, e^{-\mu z}(\cos \mu z + \sin \mu z) \tag{48}$$

$$\tau_{\xi\eta}(\text{membrane}) = -\tfrac{1}{4}(1+\lambda^2\sin^2\theta)^{-1}[e^{-\mu z}\cos\mu z\{\sin\theta(2\lambda+\lambda^3)-\lambda^3\sin 3\theta\} + \lambda^3 e^{-4z/\beta}\cos(4z/\beta)(\sin 3\theta-\sin\theta)] \quad (49)$$

$$\sigma_\xi(\text{bending}) = \frac{3\beta\lambda\cos\theta}{[12(1-\nu^2)]^{\frac{1}{2}}}e^{-\mu z}(\cos\mu z-\sin\mu z) \quad (50)$$

$$\sigma_\eta(\text{bending}) = \frac{3\nu\beta\lambda\cos\theta}{[12(1-\nu^2)]^{\frac{1}{2}}}e^{-\mu z}(\cos\mu z-\sin\mu z) \quad (51)$$

$$\tau_{\xi\eta}(\text{twisting}) = \frac{3(1-\nu)}{2(1+\lambda^2\sin^2\theta)[12(1-\nu^2)]^{\frac{1}{2}}}[e^{-\mu z}\sin\mu z\{\lambda^3\sin 3\theta-\sin\theta(2\lambda+\lambda^3)\} + \lambda^3 e^{-4z/\beta}\sin(4z/\beta)(\sin 3\theta-\sin\theta)]. \quad (52)$$

Equations (50)–(52) refer to outer surface of the shell. In order to get the complete solution, we have to add the uniform stresses due to internal pressure from equations (44)–(46) to those due to the residue problem from equations (47)–(52).

If λ^2 is neglected when compared to unity for small values of α, the solution derived here becomes identical with those given in references [4] and [5].

Let us now compare the results with Van der Neut's solution. It should be mentioned here that Van der Neut's method is different from the one used in this analysis and the final solution is given in terms of $(\bar{z}, \bar{\theta})$. In comparing the two solutions, it should be kept in mind that the solution for residue stresses, given by equations (47)–(52), is valid only for $z = 0(1/\beta)$ and in this zone $\bar{\theta} \simeq \theta$ and $\bar{z} \simeq z\cos\psi$. If the slowly decaying stresses are omitted altogether and replaced by

$$N_x = \tfrac{1}{2}\lambda^2\cos 2\theta \quad (53)$$

this solution then reduces to Van der Neut's solution [3]. Equation (53), as it was mentioned earlier, is inadmissible; because it leads to a violation of the governing equations.

From equations (44), (45), (47), (48), (50) and (51), it can be observed that the non-dimensional principal stresses are functions of three parameters α, β and ν. In Figs. 6–9, the principal stresses at $z = 0$ are plotted in terms of α and β for $\nu = 0{\cdot}3$. These figures show that the stresses are more critical on the outer surface, because the membrane and bending stresses have the same sign.

The principal stresses reach their maximum values on the outer surface at $\theta = 0$ and $z = 0$, a point which is often called "Crotch". The stress concentration factor can, therefore, be based on the stress values at this point. We now define a stress concentration factor K as the ratio of an equivalent stress σ_e to the hoop stress at $z = \infty$, where the equivalent stress σ_e, based on distortion energy, is given in terms of the principal stresses σ_1 and σ_2 by

$$\sigma_e^2 = \sigma_1^2-\sigma_1\sigma_2+\sigma_2^2$$

It can be shown that K is a function of only two parameters, $\beta\lambda$ and ν. Figure 10 shows the stress concentration factor K plotted in terms of these two parameters. It can be seen that K is almost a linear function of $\beta\lambda$, except in a small range where $\beta\lambda$ is small. The slight non-linearity for larger values of $\beta\lambda$ cannot be seen in the graph due to the scale chosen.

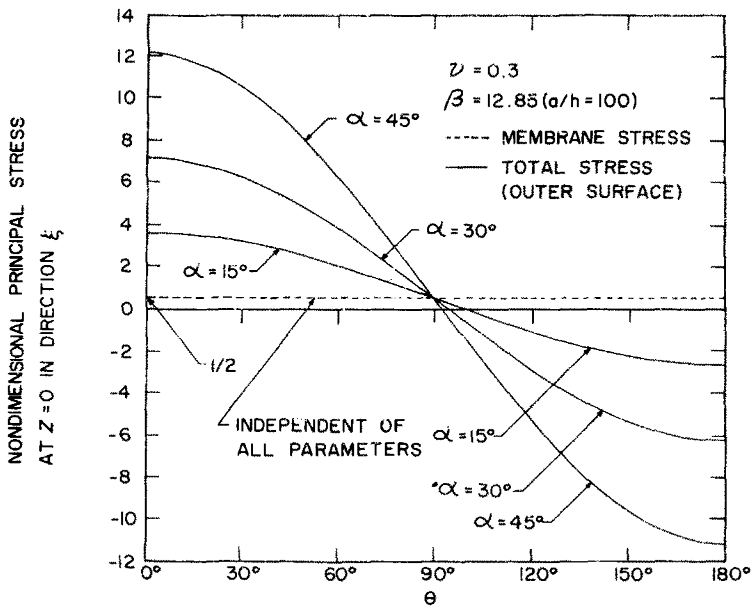

FIG. 6 Principal stress in ξ direction vs. α.

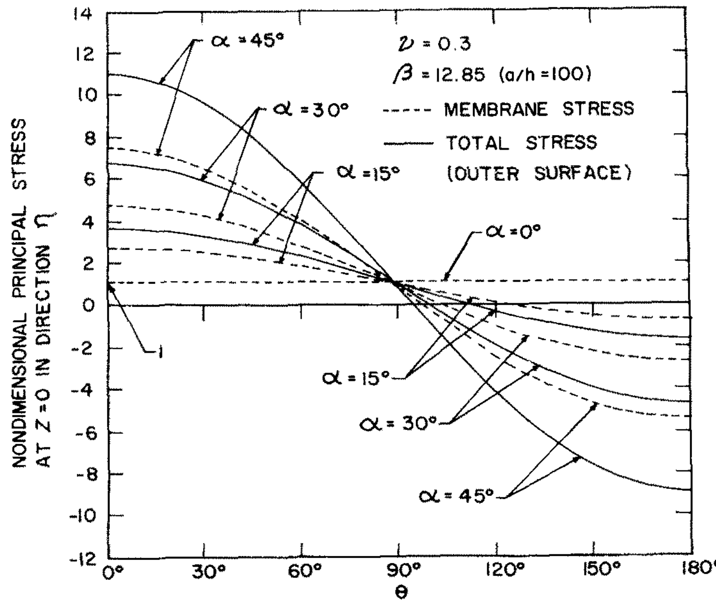

FIG. 7. Principal stress in η direction vs. α.

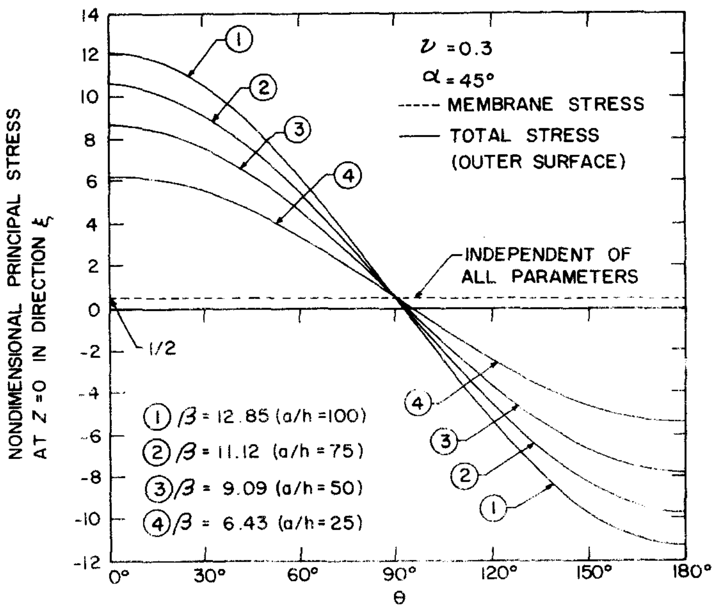

FIG. 8. Principal stress in ξ direction vs. β.

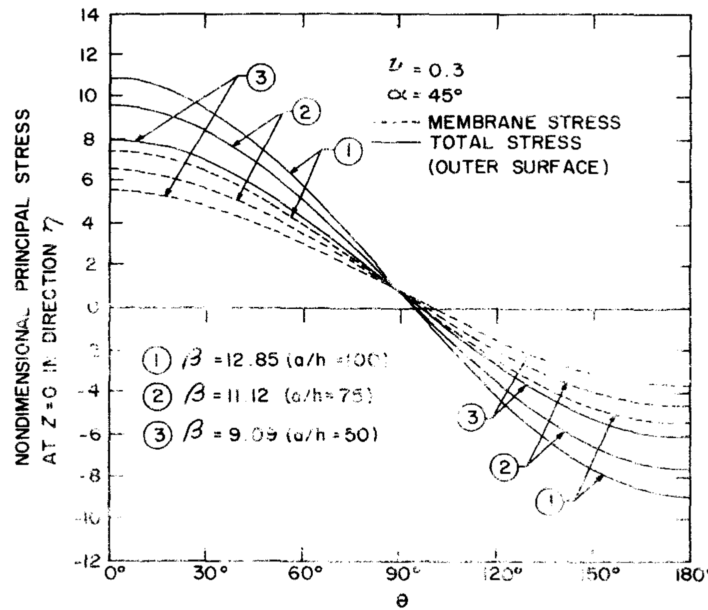

FIG. 9. Principal stress in η direction vs. β.

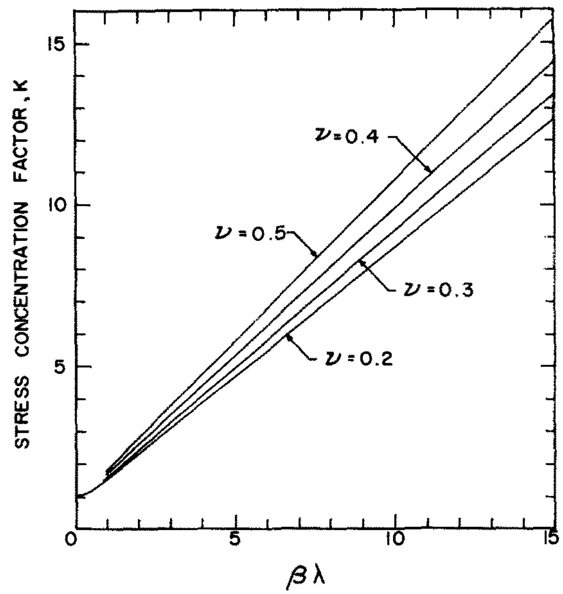

FIG. 10. Stress concentration factor plotted as a function of $\beta\lambda$ and ν.

5. CONCLUDING REMARKS

The first approximation results presented in this analysis include errors of order $(h/a)^{\frac{1}{2}}$. For instance, this would mean an error of about 10 per cent for a shell whose diameter to thickness ratio is 200. This degree of accuracy is quite good from engineering point of view, particularly in view of the fact that it is usually very difficult to arrive at simple closed form solutions in such problems. A second approximation solution, for the same diameter to thickness ratio, would mean an error of about 1 per cent which, for all practical purposes, might be considered to be a completely satisfactory solution. One might be now tempted to think that it might be worthwhile proceeding to a second approximation. In fact, considerable time was spent in trying to arrive at a second approximation solution. Unfortunately, it was found that certain equations cannot be integrated in a closed form as in the first approximation. The analysis was not continued further, because the object of this entire investigation is to arrive at closed form solutions.

Acknowledgements—The author wishes to acknowledge with gratitude the help received from G. S. Dwarakanath through many helpful discussions during the course of this work.

REFERENCES

[1] A. KORNECKI, The state of stress and strain in a thinwalled tube rigidly fixed in an oblique cross section (in Polish). *Rozpr. inż.* **5**, 119–134 (1957).

[2] J. M. CORUM, A theoretical and experimental investigation of the stresses in a circular cylindrical shell with an oblique edge. *Nucl. Engng Design* **3**, 256–280 (1966).

[3] A. VAN DER NEUT, Bending at the oblique end section of cylindrical shells. *Proc. Symp. on The Theory of Thin Elastic Shells, Delft*, 24–28 *August* 1959, pp. 247–269. North Holland (1960).

[4] A. E. GREEN and W. C. EMMERSON, Stresses in a pipe with a discontinuous bend. *J. Mech. Phys. Solids* **9**, 91–104 (1961).

[5] M. V. V. MURTHY, Stresses in a mitred pipe joint under uniform internal pressure. *Int. J. mech. Sci.* **6**, 361–370 (1964).
[6] L. H. DONNEL, *NACA Report No.* 479, Washington, D.C. (1933).
[7] A. L. GOL'DENVEIZER, *Theory of Elastic Thin Shells*, p. 366. Pergamon (1961).

(*Received* 14 *October* 1968; *revised* 24 *February* 1969)

Абстракт—Приводится расчет напряжений в месте соединения двух цилиндрических оболочек одинакого диаметра. Соединение образует плоской эллиптический торец. Оболочки подвергаются внутреннему давлению. Результаты справедливы для всех возможных значений угла между осями этих двух оболочек. Допускаются погрешности порядка $(h/a)^{\frac{1}{2}}$, где h и a обозначают, соответственно, толщину и радиус оболочки. Даются результаты в виде простых формул для напряжений вблизи плоскости соединения. Приводится график, из которого можно непосредственно отсчитать фактор концентрации напряжений, основанный на энергии дисторсии, для широкого рода параметров.